Journal of Cluster Science (2018) 29:967–974
https://doi.org/10.1007/s10876-018-1406-2

ORIGINAL PAPER

Photoluminescence and Magnetism Study of Blue Light Emitting the Oxygen-Bridged Open-Cubane Cobalt(II) Cluster

Elif Gungor[1] · Mustafa Burak Coban[1,2] · Hulya Kara[1,3] · Yasemin Acar[1]

Received: 1 April 2018 / Published online: 2 June 2018

Abstract

A new cubane-based cobalt(II) cluster, $[Co_4L_4]$ (**1**), where H_2L = 2-((E)-(2-hydroxyethylimino) methyl)-4-chlorophenol has been prepared using a solvothermal process and characterized by structural, optical and magnetism. The crystal structure of **1** consists of a tetranuclear Co_4O_4 core in an open-cubane framework. Each cobalt(II) ion is penta-coordinated in a distorted square pyramidal geometry ($\tau_{Co1=Co1i}$ = 0.030, $\tau_{Co2=Co2i}$ = 0.023). Furthermore, the photoluminescence analysis indicates that **1** has a strong blue emission which should be attributed to coordination of the metal to the ligand. The temperature dependence of the magnetic susceptibilities of **1** shows antiferromagnetic coupling (J = − 26.61 ± 0.01) between cobalt(II) ions.

Keywords Schiff base · Open-cubane Co(II) cluster · Photoluminescence · Antiferromagnetic interaction

Introduction

The design, synthesis, and characterization of polynuclear transition metal complexes have attracted considerable attention in the development of coordination chemistry [1, 2], molecular magnetism [3, 4], bioinorganic chemistry [5]. These complexes have unique chemical and physical properties as photocatalysts for water oxidation [6, 7] single-molecule magnets (SMMs) [8, 9], biological activities [10–12], catalysis [13, 14] and modeling biochemical reactions [15, 16]. Moreover, these complexes show photoluminescent and electroluminescent properties due to electron transport, light emission, higher thermal stability and their ease of sublimation [17–20]. They are widely used as light emitting materials and an electron transporting materials in organic light emitting diodes (OLED) applications [21–23]. Their optical properties can be easily adjusted through the coordinated metal center or modify of the substituents of ligands.

Cobalt complexes containing Co_4O_4 cores have been classified in the literature as butterfly, incomplete cubane, cubane, defect dicubane topologies [24–29]. Cobalt complexes in these topologies have been extensively studied in terms of structural, spectroscopic, biological and magnetic properties through experimental and theoretical approaches [24–32]. So far, the structural and magnetic characterization of cubane-based cobalt(II) complexes have been published by various research groups [33–36]. But, studies on the solid-state photoluminescence properties of open-cubane cobalt (II) complexes have been limited number in the literature [37].

Previously, our research group and others have studied on structural and magnetic and photoluminescence characterization of mono, binuclear, trinuclear and tetranuclear complexes containing Schiff base ligands and transition metal ions [29, 38–45]. For enlarge the library of cubane-based cobalt (II) clusters, we describe here the crystal structure, photoluminescence and magnetic properties of a new open-cubane cobalt (II) cluster.

Electronic supplementary material The online version of this article (https://doi.org/10.1007/s10876-018-1406-2) contains supplementary material, which is available to authorized users.

✉ Elif Gungor
elifonly@gmail.com

✉ Hulya Kara
hkara@balikesir.edu.tr

[1] Department of Physics, Faculty of Science and Art, Balikesir University, 10145 Balikesir, Turkey

[2] Center of Science and Technology Application and Research, Balikesir University, 10145 Balikesir, Turkey

[3] Department of Physics, Faculty of Science, Mugla Sitki Kocman University, 48170 Mugla, Turkey

Experimental

Materials and Instrumentation

5–chlorosalicylaldehyde, ethanolamine, metal salt and solvents in the synthesis were used in the reagent grade and without any purification. UV–Vis spectra in solid-state were measured by an Ocean Optics Maya 2000–PRO spectrometer. Infrared spectra were recorded on a Perkin–Elmer Spectrum 65 instrument (4000–600 cm^{-1}). Powder X-ray measurements were performed on a Bruker–AXS D8–Advance diffractometer using Cu–K_α radiation (λ = 1.5418 Å) in the range $5° < 2\theta < 50°$ in $\theta-\theta$ mode with a step time of ns (5 s < n < 10 s) and step width of 0.02°. Solid-state photoluminescence spectra were measured with an ANDOR SR500i–BL Photoluminescence Spectrometer. The measurements were done by using excitation source (349 nm) of a Spectra–physics Nd:YLF laser with a 5 ns pulse width and 1.3 mJ of energy per pulse as the source. Magnetic measurements were performed by a QD model SQUID magnetometer at a field of 1.0 T.

Synthesis of H_2L and 1

The ONO type Schiff base ligand, **H_2L** 2-((E)-(2-hydroxyethylimino) methyl)-4-chlorophenol, was prepared from ethanolamine (1 mmol, 0.061 mL) and 5–chlorosalicylaldehyde (1 mmol, 0.156 g) in a 1:1 molar ratio in hot methanol (60 cm^3) according to the method reported previously [11]. The solution obtained was stirred at 65 °C for 15 min. The yellow compound precipitated from the solution on cooling. Analysis calculated for $C_9ClNH_{10}O_2$ (Yield 80%): C, 54.15; H, 5.05; N, 7.02%; Found: C, 54.11; H, 4.98; N, 7.06%.

A methanol solution (20 mL) of cobalt(II) acetate tetrahydrate (1 mmol, 0.249 g) was added to a methanol solution (30 mL) of the ligand, H_2L (1 mmol, 0.199 g). The mixture was heated to 65 °C with stirring for 15 min and then, triethylamine (Et_3N) (1 mmol, 0.101 mL) was added to the solution. The resulting red solution was stirred for a further 10 min, filtered, and then allowed to stand at room temperature. Red block crystals were obtained after 4 days. Analysis calculated for $C_{36}H_{32}Cl_4Co_4N_4O_8$, CH_3OH (Yield 70%): C 41.99, H 3.43, N 5.29%; Found: C 41.95, H 3.48, N 5.25%.

The synthetic route of **1** is outlined in Scheme 1. In the presence of added bases, such as NaOH or NEt_3, high-nuclearity cubane-type clusters have a tendency to form. In the formation of the complex **1**, the Schiff base ligand, H_2L is deprotonated and then coordinated to the Co(II) atoms. This process commonly occurs during the formation of polynuclear metal complexes [34, 45–47].

X-ray Structure Determination

Diffraction measurements were made at a Bruker Apex II Kappa CCD diffractometer using monochromatic Mo–K_α radiation at 100 K [48]. The structure was solved by direct methods in the OLEX2 program [49], using SHELXS [50] and refined by full–matrix least–squares based on $|F_{obs}|^2$ using SHELXL [51]. The non–hydrogen atoms were refined anisotropically. The hydrogen atoms were included in the structure factor calculations at idealized positions and were allowed to ride on their parent atoms. The solvent methanol molecule in the crystal lattice appears to be highly disordered. Therefore, to eliminate the electron intensity contributions from the disordered solvent molecules was used to OLEX2 [44] solvent mask function. The final refinement of the structure of **1** was carried out using the intensities modified by the Olex2 solvent mask. The methanol molecule and their hydrogen atoms were not included in the total atomic formula and they are not included in the list of atoms. Thirty missing reflections appeared to be obscured by the beamstop, thus reducing the completeness to less than 100%. The twenty-eight reflections were omitted from the refinement owing to bad disagreement. Crystal data and structural refinement parameters for **1** are given in Table 1. The geometric parameters are listed in Table 2. CCDC 826649 contains the crystallographic data for the structural analyses of **1**. These data can be obtained free of charge via www.ccdc.cam.ac.uk.

Results and Discussion

Crystal Structure

Complex **1** crystallizes in the orthorhombic space group *Pbcn*. Its asymmetric unit consists of one $[Co^{II}_2L_2]$ subunit. Crystal structure determination indicates that **1** is a cubane-based structure consisting of two dinuclear $[Co^{II}_2L_2]$ subunits (Fig. 1). The four cobalt (II) ions are linked by μ_3-alkoxo bridges, generating an open-cubane type $\{Co_4O_4\}$ configuration. The oxidation states of cobalt atoms are determined by bond-valence method (or bond valence sum) [52, 53]. As seen in Table 2, the bond-valence-sum reconfirms the valence state 2 +.

Each cobalt (II) ion is pentacoordinate by one imine nitrogen atom, one phenoxy oxygen atoms and three μ_3-alkoxo oxygen atoms from the Schiff base ligands. The Addison distortion indexes of Co1($Co1^i$) and Co2($Co2^i$) atoms were found to be $\tau_{Co1=Co1i}$ = 0.030,

Scheme 1 The synthetic route of **1**

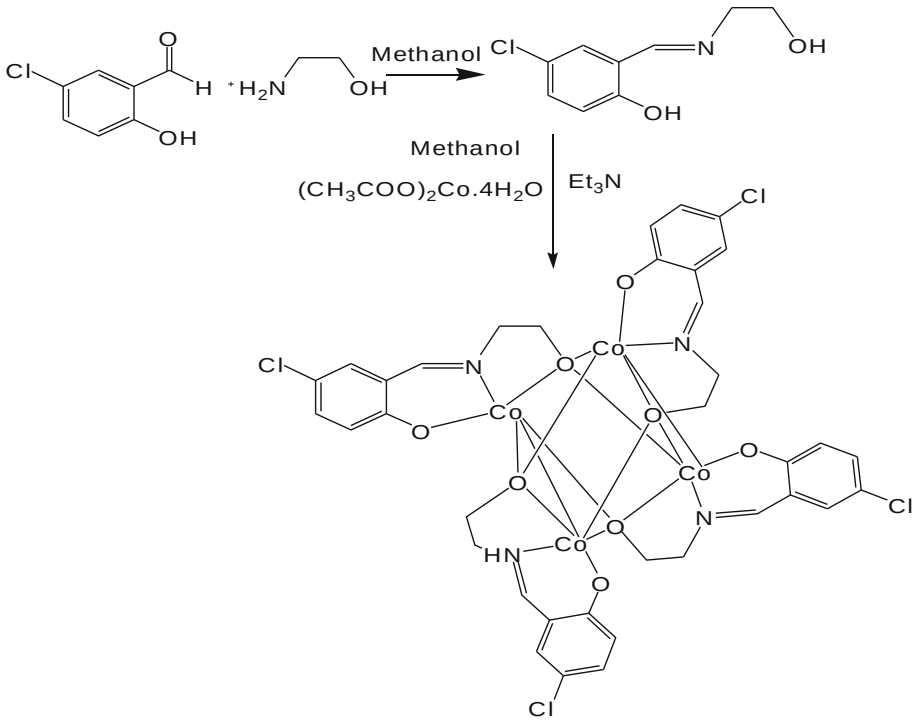

Table 1 Crystal data and structure refinements for **1**

Empirical formula	$C_{36}H_{32}Cl_4Co_4N_4O_8$
Formula weight	1026.18
Crystal system	Orthorhombic
Space group	*Pbcn*
a	19.0292 (3) Å
b	21.9494 (4) Å
c	9.4152 (2) Å
α = β = γ	90°
Volume	3932.54(13) $Å^3$
Z	4
ρ_{calc}	1.733 g/cm^3
μ	1.986 mm^{-1}
Θ range for data collection	1.4°–27.6°
Index ranges	$-21 \le h \le 24$
	$-28 \le k \le 25$
	$-5 \le l \le 12$
Reflections collected	19,500
Independent reflections	4504
Data/restraints/parameters	4504/6/253
Goodness-of-fit on F^2	1.26
Final R indexes [I ≥ 2σ (I)]	R_1 = 0.074, wR_2 = 0.162

Table 2 Selected geometric parameters (Å, °) for **1** and bond valance sum (BVS) calculations for the Co ions

Co1–O3	1.900 (5)	Co2–O2	1.902 (6)
Co1–O1	1.952 (4)	Co2–O4^i	1.963 (4)
Co1–O4	1.978 (5)	Co2–O1	1.974 (4)
Co1–N2	1.944 (6)	Co2–N1	1.934 (5)
Co1–O4^i	2.432(4)	Co2–O1^i	2.419(5)
O1–Co1–O3	94.03 (2)	O1–Co2–O2	176.4 (2)
O3–Co1–O4	176.0 (2)	O4^i–Co2–O1	87.15 (2)
O1–Co1–O4	89.0 (2)	Co1–O1–Co2	105.4 (2)
O2–Co2–O4^i	94.9 (2)	Co2^i–O4–Co1	101.8 (2)
	The oxidation state of Co		
	2+		
Co1 (Co1^i)	2.14		
Co2 (Co2^i)	2.10		

Symmetry codes: (i) $-x, y, -z + 3/2$

$\tau_{Co2=Co2i}$ = 0.023, respectively (i = $-x$, y, $-z + 3/2$) [54]. Therefore, the coordination polyhedron of each cobalt (II) center is described as distorted square pyramidal. The basal plane of the square pyramid is constructed by NO_3 atoms, whereas the apical position is occupied by a μ_3-alkoxo oxygen atom. Co1 (Co1^i) and Co2 (Co2^i) for **1** deviate from the NO_3 basal planes by 0.428 and 0.345Å towards the apical ligand atom. The basal Co–O bond distances are in the range of 1.900 (5)–1.978 (5) Å, while the axial bond distances range of 2.419 (5)–2.432 (4) Å. The basal Co–N bond distances and Co–O_{alkoxo}–Co bridging bond angles are 1.934 (5)–1.944 (6) Å and 101.8 (2)–105.4 (2)°, respectively. Co···Co distances vary from

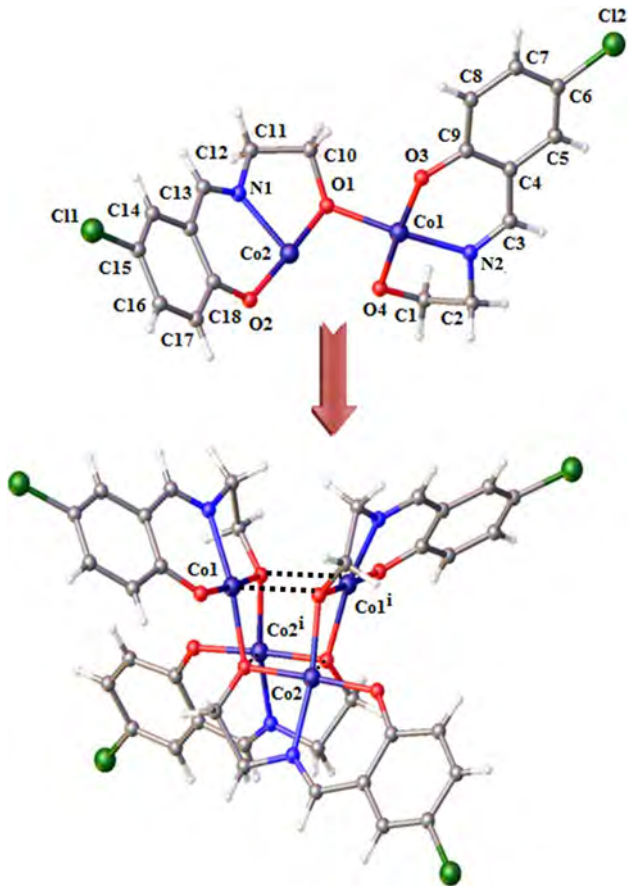

Fig. 1 Molecular structure of **1** (i = − *x*, *y*, − *z* + 3/2)

3.059 (1) to 3.466 (1) Å. All bond distance and angles resemble in those reported earlier structures [37, 55].

In the crystalline architecture of **1**, adjacent tetranuclear molecules are connected by C16–H16···O2 and C11–H11A···Cl1 hydrogen bonds which lead to a hydrogen-bonded two-dimensional structure in the *ac* plane (Table 3, Fig. 2). This structure lies in *a*-axis and stacks along to the *c*-axis (Fig. 3). Besides, intermolecular π···π and C–H···π ring interactions are observed between benzene rings (Fig. 3, Table 3).

Before performing the characterization of the complex, the experimental and simulated powder X-ray diffraction patterns of **1** are compared as seen Fig. S1. The experimental PXRD patterns are in good agreement with the simulated patterns on single crystal X-ray structure.

FT-IR Spectra

The shifts in the important vibrational bands of the azomethine $\nu_{(C=N)}$, $\nu_{(C-O)}$, phenolic $\nu_{(O-H)}$, $\nu_{(C-O)}$ and $\nu_{(C-H)}$ groups are shown in Fig. S2 and Table S1. A broad band in the range of 3494–3269 cm^{-1} which corresponds to the aromatic $\nu_{(O-H)}$ stretching vibration, can be connected with the presence of OH^- a chelating group within the structure of the complex. The bands centered in the range of 2907–2884 cm^{-1} may be associated with the stretching vibrations of the aromatic and aliphatic C–H bonds. The strong band at 1647 cm^{-1} assigned to $\nu_{(C=N)}$ in the free ligand, shifted to lower wavenumber (1643 cm^{-1}) in **1**. This shift shows the participation of the azomethine nitrogen in metal coordination [56]. The band of $\nu_{(C-O)}$ vibrations in the free ligand is at 1278–1215 cm^{-1} while the band of $\nu_{(C-O)}$ vibrations of **1** has shifted to a lower frequency (1268–1209 cm^{-1}) which is confirmed the presence of phenolic oxygen in the coordination. The characteristic band of $\nu_{(C-Cl)}$ vibrations of $\mathbf{H_2L}$ and **1** is in the range of 729–615 cm^{-1} [40, 57].

Solid State UV–Vis Spectra

A solid-state electronic absorption spectral data of **1** and its free ligand $\mathbf{H_2L}$ was recorded (Fig. S3). The data are summarized in Table S1. The absorption spectra of **1** display different absorption pattern as compared to $\mathbf{H_2L}$. The electronic spectral data of $\mathbf{H_2L}$ exhibit two bands in the UV region at 302 and 437 nm while its cobalt (II) complex

Table 3 Hydrogen bond and short-contact geometry (Å, °) for **1**

D–H···A*	D–H	H···A	D···A	D–H···A	Symmetry
C16–H16···O2	0.95	2.55	3.476 (8)	165	− 1/2 − x, 1/2 − y, − 1/2 + z
C11–H11A···Cl1	0.98	2.88	3.69 (8)	139	− x, y, 1/2 − z
Cg(I)···Cg(J)	Cg(I)···Cg(J)	*Ring centroid*			
Cg (5) ···Cg (6)	3.610(4)	Cg (5) = C5–C6–C7–C8–C9			1/2 + x, 1/ − y, 1 − z
		Cg(6) = C13–C14–C15–C16–C17–C18			
X–H···Cg(I)	X–H···Cg(I)	X···Cg(I)			
C3–H3···Cg (5)	161	3.789 (8)			x, 1 − y, 1/2 + z

**D* Donor, *A* Acceptor, *M* Metal, *Cg(I)* plane number I (ring number in () above), *Cg–Cg* distance between ring centroids (Å)

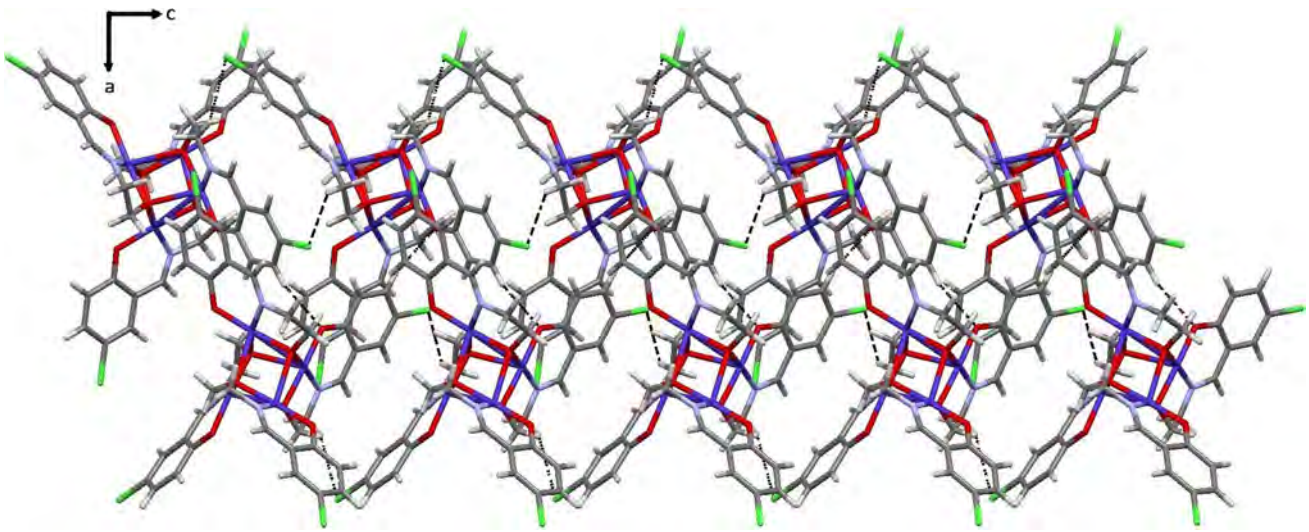

Fig. 2 2-D structure of **1** showing the intermolecular C16–H16···O2 and C11–H11A···Cl1 hydrogen bonds

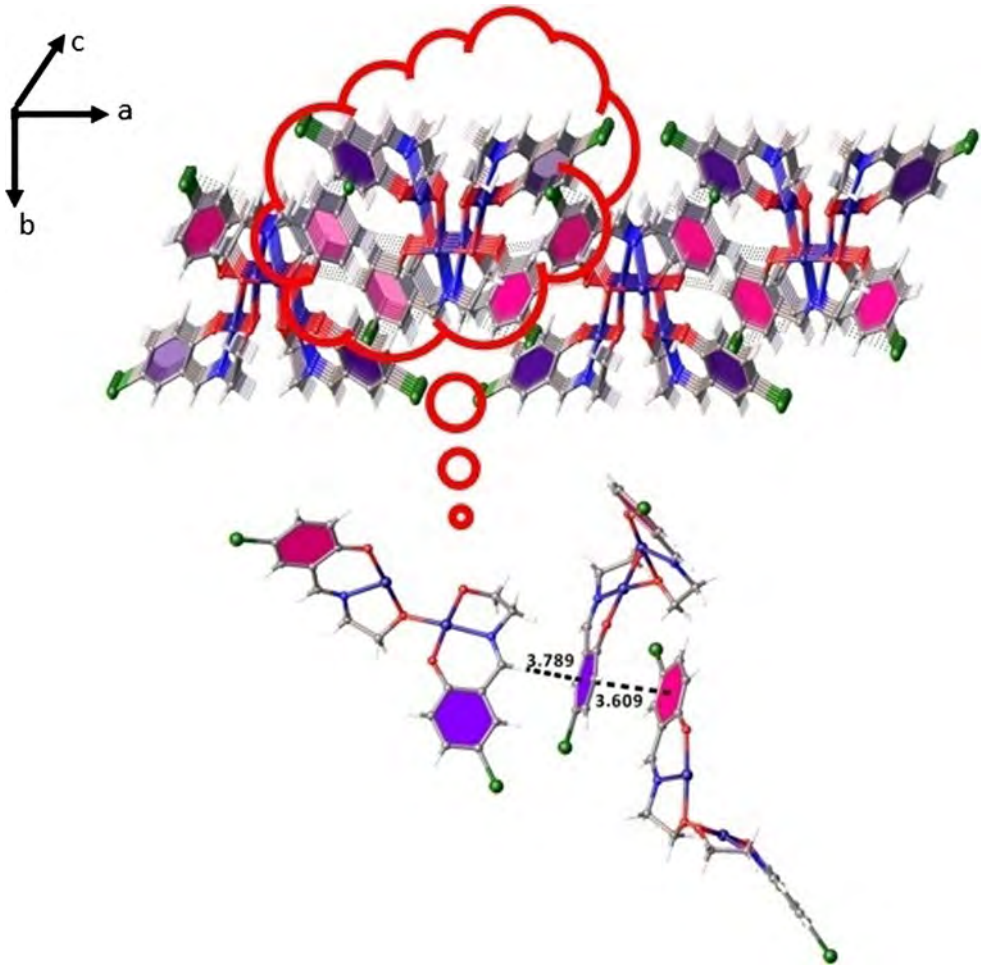

Fig. 3 The hydrogen-bonded 2D structure lies in *a*- axis and stacks along to the *c*-axis. The intermolecular π ···· π and C–H ··· π ring interactions in **1**

show absorption bands at 333 and 470 nm. These absorption bands of **1** are assigned to the π → π* and n → π* electronic transitions of the azomethine and the carbonyl groups [58]. In addition, the shifting of the absorption band in the spectra of the complex towards longer wavelength compared to that of its ligand, which is signified the metal ion coordination with the ligand [58, 59].

Solid State Photoluminescence Properties

The solid-state photoluminescence (PL) spectroscopy of **1** and its free ligand **H_2L** was investigated in the visible region at room temperature. As seen from Fig. 4, **H_2L** indicates a strong green emission band at λ_{max} = 505 nm, which is attributable to the n→π or π→π* electronic transition (ILCT) [60, 61] and **1** has a strong blue emission band at λ_{max} = 472 nm and moderate emission band at λ_{max} = 694 nm. The observed blue shift of the stronger emission bands of **H_2L** and **1** is due to the complexation of the metal ion with the ligand [40, 62]. Besides, the intensity emission of **1** is found to be higher than intensity emission of its free ligand. As described earlier, the rigidity of the ligand after coordination with the metal ions reduces the loss of energy by radiation-less decay which resulted in comparatively sharp emission peaks [63].

Magnetic Properties

The DC magnetic susceptibility for **1** was performed between 2 and 300 K under a magnetic field of 1000 Oe and the plot of $\chi_m T$ versus T is shown in Fig. 5. The experimental $\chi_m T$ value at 300 K is 11.30 cm^3 K mol^{-1}, which is higher than the spin-only value of 7.50 cm^3 $Kmol^{-1}$ for a tetranuclear cobalt (II) (S = 3/2, g = 2.0) system. This can be explained by the orbital contribution to the magnetic moment of the cobalt(II) ions [34, 35]. With decreasing T, the $\chi_m T$ value decreases to reach a minimum value of 0.135 cm^3 K mol^{-1} at 2 K. This feature indicates the presence of an antiferromagnetic interaction between cobalt(II) ions [36]. The magnetic exchange analysis for cobalt(II) complexes is difficult due to orbital contribution to the magnetic moment [34, 35]. In this respect, the magnetic susceptibility data can be fit by Eq. (1), based on the isotropic spin Hamiltonian $H = -2J(S_1S_2)$,

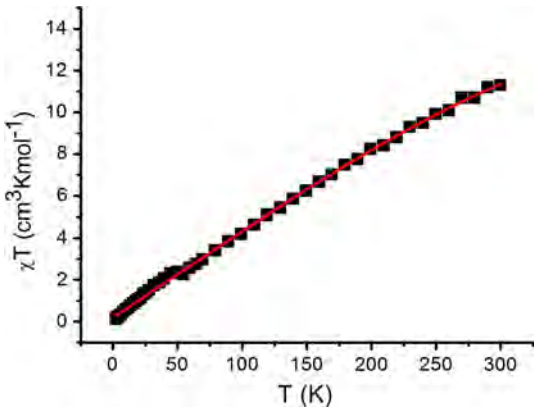

Fig. 5 Temperature dependence of $\chi_M T$ versus T for **1**. The solid red line represents the best fit

$$\chi_m T = \frac{2Ng^2\beta^2}{k}\frac{(9e^{2J/kT} + 55e^{6J/kT} + 140e^{12J/kT} + 180e^{20J/kT} + 165e^{30J/kT} + 91e^{42J/kT})}{(4 + 27e^{2J/kT} + 55e^{6J/kT} + 70e^{12J/kT} + 54e^{20J/kT} + 33e^{30J/kT} + 13e^{42J/kT})}(1-\rho) + \frac{2Ng^2\beta^2}{k}\rho + N_\alpha \quad (1)$$

where N, g, μ_B, k, T have their usual meanings, ρ is the fraction of paramagnetic impurity and N_α is the temperature independent paramagnetism. The best-fit parameters obtained are as follows: g = 2.50 ± 0.01, J = –26.61 ± 0.01, ρ = 0.03 ± 0.01, $N_\alpha = 600 \times 10^{-6}$.

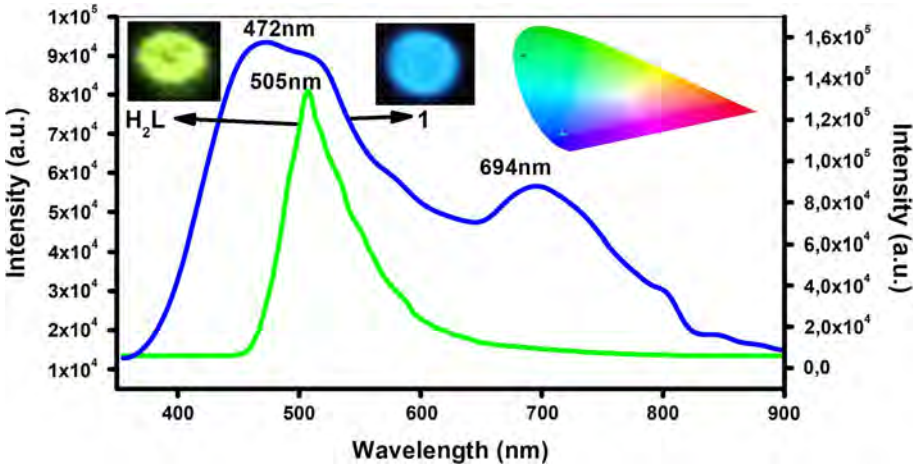

Fig. 4 The emission spectrum of **H_2L** and **1** at room temperature ($\lambda_{exc.}$ = 349 nm)

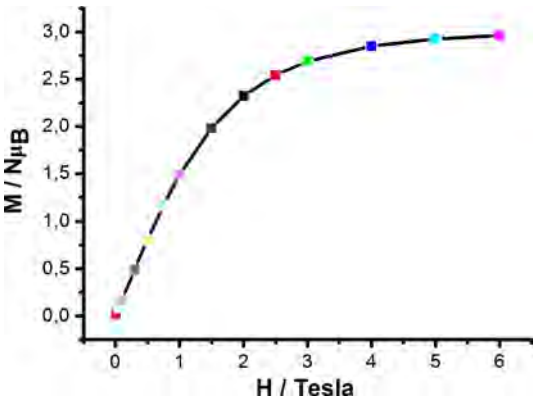

Fig. 6 Magnetization as a function of the applied magnetic field for **1**, performed at 4.5 K

The open-cubane structure adopted in Co_4L_4 (**1**) is an unusual motif, but the magnetic properties of several such cubane cobalt(II) clusters have been studied. Both ferromagnetically [64, 65] and antiferromagnetically [66, 67] coupled systems have been reported. The Co–O–Co bridging angle in cubane cobalt(II) complexes found a crucial role on the sign and magnitude of the exchange interaction [33, 44]. The exchange interaction is antiferromagnetic for Co–O–Co bridging angles larger than around 99° and ferromagnetic for small angles [44].

In the case of our cluster **1,** the Co–O–Co bridging angles are 101.8 (2) and 105.4(2)°, which are greater than the crossover angle, the expected coupling through this bridge should be antiferromagnetic for **1**.

The field dependence of the magnetization for **1** has been measured at 4.5 K. The magnetization plot shows that the magnetization exhibits a steady increase with the increase of the applied magnetic field, which agrees with the assumption of the antiferromagnetic exchange interactions (Fig. 6). The magnetization reach at 2.96 NμB value at 6 T which is smaller than the S = 3/2 saturation value, (3.76 $N\mu_B$) (assuming S = 3/2, g = 2.51), probably due to the zero-field splitting of Co(II) [36].

Conclusions

In this work, crystal structure, photoluminescence and magnetic properties of a new open-cubane cobalt (II) complex have been reported. DC magnetic properties of **1** are in good agreement with the literature. $\chi_M T$ versus T curve was fitted with the isotropic spin Hamiltonian model and the best-fit parameters show antiferromagnetic interaction in the complex. The solid-state photoluminescence measurements of **1** indicate blue light emissions while its ligand $\mathbf{H_2L}$ display green light emission which can be associated with the $n\rightarrow\pi$ or $\pi\rightarrow\pi^*$ electronic transition (ILCT). Hence, the results show that synthesized cobalt (II) complex can be used as a promising emission source for blue organic light-emitting devices application.

Supporting Information

The figures of X-ray powder diffraction, UV–Vis and FTIR spectroscopies are provided as supporting information.

Acknowledgements The authors are grateful to the Research Funds of Balikesir University (BAP–2017/199) for the financial support and Balikesir University, Science and Technology Application and Research Center (BUBTAM) for the use of the Photoluminescence Spectrometer. The authors are also very grateful to Prof. Dr. Andrea Caneschi (Laboratory of Molecular Magnetism, Department of Chemistry, University of Florence) for the use of SQUID magnetometer and helpful suggestions.

References

1. S. G. Kang, H. Kim, S. Bang, and C. H. Kwak (2013). *Inorg. Chim. Acta* **396**, 10.
2. C. J. Adams, M. A. Kurawa, M. Lusi, and A. G. Orpen (2008). *CrystEngComm* **10**, 1790.
3. O. Kahn *Molecular Magnetism* (VCH Publishers, New York, 1993).
4. A. Mukherjee, R. Raghunathan, M. K. Saha, M. Nethaji, S. Ramasesha, and A. R. Chakravarty (2005). *Chem. A Eur. J.* **11**, 3087.
5. W. Kaim and B. Schwerderski *Bioinorganic Chemistry: Inorganic Elements in the Chemistry of Life* (John Wiley, Chichester, 1994).
6. K. Dimitrou, K. Folting, W. E. Streib, and G. Christou (1993). *J. Am. Chem. Soc.* **115**, 6432.
7. W. F. Ruettinger, D. M. Ho, and G. C. Dismukes (1999). *Inorg. Chem.* **38**, 1036.
8. E. C. Yang, D. N. Hendrickson, W. Wernsdorfer, M. Nakano, L. N. Zakharov, R. D. Sommer, A. L. Rheingold, M. Ledezma-Gairaud, and G. Christou (2002). *J. Appl. Phys.* **91**, 7382.
9. C. J. Milios, A. Vinslava, P. A. Wood, S. Parsons, W. Wernsdorfer, G. Christou, S. P. Perlepes, and E. K. Brechin (2007). *J. Am. Chem. Soc.* **129**, 8.
10. S. Celen, E. Gungor, H. Kara, and A. D. Azaz (2016). *Mol. Cryst. Liq. Cryst.* **631**, 164.
11. E. Gungor, S. Celen, D. Azaz, and H. Kara (2012). *Spectrochim. Acta—Part A Mol. Biomol Spectrosc.* **94**, 216.
12. H. F. Abd El-Halim and G. G. Mohamed (2018). *Appl. Organomet. Chem.* **32**, e4176.
13. C. Ni, E. E. Knyazeva, I. F. Moskovskaya, and B. V. Romanovsky (2001). *Polyhedron* **20**, 915.
14. R. Chakrabarty, S. J. Bora, and B. K. Das (2007). *Inorg. Chem.* **46**, 9450.
15. G. Christou (1989). *Acc. Chem. Res.* **22**, 328.
16. S. Mukhopadhyay, S. K. Mandal, S. Bhaduri, and W. H. Armstrong (2004). *Chem. Rev.* **104**, 3981.
17. S. Konar, A. Jana, K. Das, S. Ray, S. Chatterjee, J. A. Golen, A. L. Rheingold, and S. K. Kar (2011). *Polyhedron* **30**, 2801.
18. A. Majumder, G. M. Rosair, A. Mallick, N. Chattopadhyay, and S. Mitra (2006). *Polyhedron* **25**, 1753.
19. T. Yu, W. Su, W. Li, Z. Hong, R. Hua, and B. Li (2007). *Thin Solid Films* **515**, 4080.

20. M. Srinivas, G. R. Vijayakumar, K. M. Mahadevan, H. Nagabhushana, and H. S. Bhojya Naik (2017). *J. Sci. Adv. Mater. Devices* **2**, 156.
21. M. Srinivas, T. O. Shrungesh Kumar, K. M. Mahadevan, S. Naveen, G. R. Vijayakumar, H. Nagabhushana, M. N. Kumara, and N. K. Lokanath (2016). *J. Sci. Adv. Mater. Devices* **1**, 324.
22. L. M. Leung, W. Y. Lo, S. K. So, K. M. Lee, and W. K. Choi (2000). *J. Am. Chem. Soc.* **122**, 5640.
23. G. Yu, Y. Liu, Y. Song, X. Wu, and D. Zhu (2001). *Synth. Met.* **117**, 211.
24. F. Sama, I. A. Ansari, M. Raizada, M. Ahmad, M. Ashafaq, M. Shahid, B. Das, K. Shankar, and Z. A. Siddiqi (2017). *J. Clust. Sci.* **28**, 1355.
25. A. Buragohain, M. Yousufuddin, M. Sarma, and S. Biswas (2016). *Cryst. Growth Des.* **16**, 842.
26. J. L. H. A. Duprey, J. Carr-Smith, S. L. Horswell, J. Kowalski, and J. H. R. Tucker (2016). *J. Am. Chem. Soc.* **138**, 746.
27. L. Jiang, D. Y. Zhang, J. J. Suo, W. Gu, J. L. Tian, X. Liu, and S. P. Yan (2016). *Dalt. Trans.* **45**, 10233.
28. L. Wen, Y. Li, D. Dang, Z. Tian, Z. Ni, and Q. Meng (2005). *J. Solid State Chem.* **178**, 3336.
29. M. B. Coban, E. Gungor, H. Kara, U. Baisch, and Y. Acar (2018). *J. Mol. Struct.* **1154**, 579.
30. I. A. Ansari, F. Sama, M. Shahid, M. Khalid, P. K. Sharma, M. Ahmad, and Z. A. Siddiqi (2016). *J. Inorg. Organomet. Polym. Mater.* **26**, 178.
31. C. N. Brodsky, R. G. Hadt, D. Hayes, B. J. Reinhart, N. Li, L. X. Chen, and D. G. Nocera (2017). *Proc. Natl. Acad. Sci.* **114**, 3855.
32. F. Evangelisti, R. Güttinger, R. Moré, S. Luber, and G. R. Patzke (2013). *J. Am. Chem. Soc.* **135**, 18734.
33. K. G. Alley, R. Bircher, H. U. Güdel, B. Moubaraki, K. S. Murray, B. F. Abrahams, and C. Boskovic (2007). *Polyhedron* **26**, 369.
34. Y. Wang, Y. Ma, R. Liu, L. Yang, G. Tian, and N. Sheng (2016). *Z. Anorg. Allg Chem.* **642**, 546.
35. S. H. Zhang, Y. D. Zhang, H. H. Zou, J. J. Guo, H. P. Li, Y. Song, and H. Liang (2013). *Inorg. Chim. Acta* **396**, 119.
36. W. B. Shi, A. L. Cui, and H. Z. Kou (2015). *Polyhedron* **99**, 252.
37. Q. Gao, Y. Qin, Y. Chen, W. Liu, H. Li, B. Wu, Y. Li, and W. Li (2015). *RSC Adv.* **5**, 43195.
38. E. Gungor and H. Kara (2012). *Inorg. Chim. Acta* **384**, 137.
39. Y. Yahsi, E. Gungor, M. B. Coban, and H. Kara (2016). *Mol. Cryst. Liq. Cryst.* **637**, 67.
40. E. Gungor (2017). *Acta Crystallogr. Sect. C Struct. Chem.* **73**, 393.
41. E. Gungor, H. Kara, E. Colacio, and A. J. Mota (2014). *Eur. J. Inorg. Chem.* **9**, 1552.
42. E. Gungor and H. Kara (2015). *J. Struct. Chem.* **56**, 1646.
43. C. Kocak, G. Oylumluoglu, A. Donmez, M. B. Coban, U. Erkarslan, M. Aygun, and H. Kara (2017). *Acta Crystallogr. Sect. C Struct. Chem.* **73**, 414.
44. G. P. Guedes, S. Soriano, N. M. Comerlato, N. L. Speziali, P. M. Lahti, M. A. Novak, and M. G. F. Vaz (2012). *Eur. J. Inorg. Chem.* **34**, 5642.
45. K. Zhang, J. Dai, Y. H. Wang, M. H. Zeng, and M. Kurmoo (2013). *Dalt. Trans.* **42**, 5439.
46. E. Loukopoulos, B. Berkoff, K. Griffiths, V. Keeble, V. N. Dokorou, A. C. Tsipis, A. Escuer, and G. E. Kostakis (2015). *CrystEngComm* **17**, 6753.
47. R. Wang, M. Hong, W. Su, and R. Cao (2001). *Acta Crystallogr. Sect. E Struct. Rep. Online* **57**, m325.
48. Bruker *APEX2, SAINT-Plus and SADABS* (Bruker AXS Inc., Madison, 2008).
49. O. V. Dolomanov, L. J. Bourhis, R. J. Gildea, J. A. K. Howard, and H. Puschmann (2009). *J. Appl. Crystallogr.* **42**, 339.
50. G. M. Sheldrick (2008). *Acta Crystallogr. A* **64**, 112.
51. G. M. Sheldrick (2015). *Acta Crystallogr. Sect. C Struct. Chem.* **71**, 3.
52. G. J. Palenik (1997). *Inorg. Chem.* **36**, 4888.
53. W. Liu and H. H. Thorp (1993). *Inorg. Chem.* **32**, 4102.
54. A. W. Addison, T. N. Rao, J. Reedijk, J. van Rijn, and G. C. Verschoor (1984). *J. Chem. Soc. Dalt. Trans.* 1349.
55. S. H. Zhang, L. F. Ma, H. H. Zou, Y. G. Wang, H. Liang, and M. H. Zeng (2011). *Dalt. Trans.* **40**, 11402.
56. S. H. Rahaman, R. Ghosh, T. H. Lu, and B. K. Ghosh (2005). *Polyhedron* **24**, 1525.
57. C. Hopa and I. Cokay (2016). *Acta Crystallogr. Sect. C Struct. Chem.* **72**, 601.
58. A. B. Lever *In Inorganic Electronic Spectroscopy. Studies in Physical and Theoretical Chemistry*, vol. 33 (Elsevier, Amsterdam, 1984).
59. S. Bibi, S. Mohammad, N. S. A. Manan, J. Ahmad, M. A. Kamboh, S. M. Khor, B. M. Yamin, and S. N. Abdul Halim (2017). *J. Mol. Struct.* **1141**, 31.
60. A. Donmez, M. B. Coban, C. Kocak, G. Oylumluoglu, U. Baisch, and H. Kara (2017). *Mol. Cryst. Liq. Cryst.* **652**, 213.
61. A. Donmez, G. Oylumluoglu, M. B. Coban, C. Kocak, M. Aygun, and H. Kara (2017). *J. Mol. Struct.* **1149**, 569.
62. G. Wu, X.-F. Wang, T. Okamura, W. Y. Sun, and N. Ueyama (2006). *Inorg. Chem.* **45**, 8523.
63. G. B. Che, C. B. Liu, B. Liu, Q. W. Wang, and Z.-L. Xu (2008). *CrystEngComm* **10**, 184.
64. A. Scheurer, A. M. Ako, R. W. Saalfrank, F. W. Heinemann, F. Hampel, K. Petukhov, K. Gieb, M. Stocker, and P. Müller (2010). *Chem. A Eur. J.* **16**, 4784.
65. J. F. Berry, F. A. Cotton, C. Y. Liu, T. Lu, C. A. Murillo, B. S. Tsukerblat, D. Villagrán, and X. Wang (2005). *J. Am. Chem. Soc.* **127**, 4895.
66. A. Scheurer, J. Korzekwa, T. Nakajima, F. Hampel, A. Buling, C. Derks, M. Neumann, L. Joly, K. Petukhov, K. Gieb, P. Müller, K. Kuepper, and K. Meyer (2015). *Eur. J. Inorg. Chem.* **2015**, 1892.
67. T. A. Hudson, K. J. Berry, B. Moubaraki, K. S. Murray, and R. Robson (2006). *Inorg. Chem.* **45**, 3549.